Color-sensitive ultrafast optical modulation and switching of terahertz plasmonic devices

Kumar, Abhishek; Srivastava, Yogesh Kumar; Manjappa, Manukumara; Singh, Ranjan

2018

Kumar, A., Srivastava, Y. K., Manjappa, M., & Singh, R. (2018). Color-Sensitive Ultrafast Optical Modulation and Switching of Terahertz Plasmonic Devices. Advanced Optical Materials, 6(15), 1800030-. doi:10.1002/adom.201800030

https://hdl.handle.net/10356/88953

https://doi.org/10.1002/adom.201800030

WILEY-VCH

Article type: Communication

Color sensitive ultrafast optical modulation and switching of terahertz plasmonic devices

Abhishek Kumar[1,2], Yogesh Kumar Srivastava[1,2], Manukumara Manjappa[1,2], and Ranjan Singh[1,2,*]

[1]Division of Physics and Applied Physics, School of Physical and Mathematical Sciences, Nanyang Technological University, Singapore 637371, Singapore
[2]Centre for Disruptive Photonic Technologies, The Photonics Institute, Nanyang Technological University, Singapore 637371, Singapore
[*]Email: ranjans@ntu.edu.sg

Two-dimensional micro-nanostructured metal films with hole arrays show promising feature such as extraordinary transmission of light. Such systems are interesting in the field of subwavelength photonics and nonlinear optics due to their high field confinement in addition to their inherent spectral scalability and frequency selective response. Several active schemes to control the extraordinary transmission have been recently demonstrated. However, these dynamic devices do not reveal any obvious color dependent modulation of the resonant transmission behavior. Here, we demonstrate color sensitive ultrafast modulation of extraordinary resonant transmission of terahertz waves through two-dimensional metallic hole arrays. Pumping the silicon beneath the metallic array with the light of different color and identical fluences exhibit significantly different ultrafast switching dynamics and modulation. The color dependent sensitivity and control of terahertz waves at an ultrafast time scale provides an extra degree of freedom that opens up new opportunities for future applications in active subwavelength optics, optoelectronics and all-optical switching of terahertz photonic devices.

The terahertz (THz) part of the electromagnetic spectrum offers exciting opportunities with its diverse application potential in spectroscopy, imaging, material characterization, chemical and biological sensing and high data rate wireless communications[1]. The lack of efficient terahertz sources, detectors and suitable optical components has restricted the large scale translation into commercial products and has led to the technological gap in the THz spectral range. Nevertheless, in recent times various breakthroughs have been achieved like high-power THz sources that has hastened the progress of THz research. However, for realizing practical application oriented devices such as filters, absorber, and polarization controller [2, 3] for efficient manipulation of THz waves are still lacking. In recent years, there has been a huge surge in THz research activities focused on bridging the missing technological link by achieving the controlled modulation of THz waves using structured and active devices. This surge in research activity has been fueled by the simplicity, spectral scalability, and narrow band response of frequency selective surfaces (FSS), which are primarily an array of subwavelength metallic thin-film micro-nanostructures that enable controlled interaction of electromagnetic waves. Based on the size of the subwavelength structures such as hole array and their periodicity, the spectral response of the FSS can be precisely engineered. In the recent years, hole arrays have been studied extensively both theoretically[4-10] and experimentally[10-17]. In visible and near-infrared regions a thin film of metal supports surface waves, known as surface plasmon polaritons (SPPs), which resonantly tunnel through the holes and show enhanced transmission[13, 18]. However, these surface waves are not supported by planar metal films at lower frequencies like THz, as at lower frequencies the conductivity of metals are too high that cause extremely weak guidance of the bounded surface waves. However, it has been shown both theoretically[19-21] and experimentally[22-24] that by perforating the metal thin film with planar periodic grooves, it is possible to realize the surface waves even at lower frequencies, provided that the dimension of the hole is smaller than the wavelength of light. These surface propagating waves mimic the dispersion relation of surface plasmon polaritons (SPPs), which

are called as *spoof plasmons*[19]. At terahertz (THz) frequencies, the enhanced transmission through two-dimensional rectangular hole array perforated on a metallic film can be well explained by the *spoof plasmon polariton* and localized resonance across the holes.[7] The concept of *spoof plasmon* allows us to realize strong coupling and confinement of THz waves and opens up a new direction to control its dispersion through the geometrical parameters of the structure. The frequency dependent transmission and high field confinement in two-dimensional periodic hole array could find applications in spectroscopy, subwavelength optics[25], and nonlinear optics[26]. Realizing enhanced transmission and active THz modulators form an important tool set for sensing, imaging, and wireless communication applications[27, 28]. Modulation by various schemes such as mechanical[29], optical[30], thermal[31], and electrical[32] have been reported. Among these, optical modulation provides higher degree of freedom and an easy access to control the THz wave by shining coherent light on active devices. However, the color sensitive ultrafast modulation and switching of terahertz plasmonic metamaterial devices has not been investigated. Our study reveals that the threshold fluence required to modulate and control the ultrafast switching time of the terahertz waves that can be tuned by changing the wavelength of the femtosecond pump beam. Such a color dependent response is important since it allows us to selectively choose the pump wavelength to achieve a specific modulation depth within an ultrafast timeframe, particularly in such applications that require extremely low fluence ultrafast operation.

In this work, we experimentally demonstrate color sensitive ultrafast all-optical modulation of THz waves through two-dimensional hole arrays patterned on thin film of aluminum (Al) fabricated on silicon on sapphire (SoS) substrates. Here silicon acts as an active material, which is photoexcited by 800 nm (1.55 eV) and 400 nm (3.1 eV) laser beam having photon energy above its energy band gap (E_g ~ 1.1 eV)[33]. The photo-generated carriers in silicon leads to the modulation of terahertz waves in terms of reducing the strength of enhanced transmission. Additionally, we observed the wavelength dependent ultrafast dynamic modulation of THz

wave through these metallic hole arrays. Photoexciting the silicon with different wavelengths but identical fluence modulates the THz waves with different modulation strengths and switching timescales. To demonstrate this experimentally, we used 400 nm and 800 nm wavelength femtosecond optical pump beam to photoexcite the silicon epilayer with identical pump fluences. In both the cases we observed different modulation depths, because pump beam of different wavelengths generates different carrier densities in silicon. The wavelength dependent sensitivity of hole arrays provides an additional degree of freedom to actively control and tune the THz waves and opens up new opportunities in various applications ranging from subwavelength optics, optoelectronics, and active THz devices. Such a color sensitive ultrafast scheme could also work at other electromagnetic domains with different material systems.

The diagram shown in Figure 1(a) highlights the central idea of this work, where the hole arrays are excited by optical pump beam of different colors (wavelengths) and probed by THz pulse. The different colors of optical pump beam represent the color sensitive modulation of THz transmission, where the THz beam is used as a probe to quantify the modulation strengths of each monochromatic pump beam of wavelength (λ) 400 nm and 800 nm. Inset picture in Fig. 1(a) shows the optical microscope image of the sample fabricated by conventional photolithography process highlighting the unit cell dimension of the sample possessing the square periodicity of $p_x = p_y = 110$ μm. Figure 1(b) shows the ultrafast carrier relaxation in the silicon epilayer, where the silicon film is photoexcited by 400 (blue line) and 800 nm (red line) pump beam respectively with fluence of 350 μJ/cm^2. The carrier dynamics reveal initial fast relaxation in the case of 400 nm pump beam. Figure 1(c) and 1(d) show the experimentally measured transmission spectra through hole arrays at different pump probe delay time, where the red and black curve represent the terahertz transmission when pump-probe delay time (τ_p) are -24 ps and 1260 ps respectively . In both situations carriers are not excited in silicon, hence we observed almost identical transmission spectra, whereas green solid line depicts the case where charge carriers have not fully relaxed (see Figure 1(b) at 765 ps). Since the charge carrier

excited in silicon modulates the THz waves, the time taken by carriers to relax back to the valance band decides the modulation/ switching speed. In our case, we observed the recovery of terahertz transmission spectra at 1.2 ns time scale, which confirms the ultrafast modulation speed.

Additionally, under the illumination of 800 nm and 400 nm pump beam with identical fluences, the time signal exhibits contrasting modulation in the amplitude of the oscillations in the THz pulse waveform (Figure 1(f) and 1(g)), where for 400 nm pump beam, the amplitude of THz signal shows much stronger damping than that for 800 nm pump beam possessing identical fluences. The contrast is clearer in Figure 1(e), where the modulation of time signal due to 800 and 400 nm optical pump beam at various pump fluences are plotted.

The hole array structures were fabricated on a silicon-on-sapphire (SoS) substrate, which consist of 600 nm thick epitaxial grown intrinsic silicon (Si) over a 460 μm thick r-cut sapphire substrate. The structures were patterned using the standard photolithography technique. First, a positive photoresist of thickness 1.5 μm was coated on SoS substrate and prebaked at 105 ºC for 1 minute. The substrate was then exposed under UV light after mask alignment. The exposed part of the photo-resist was removed by soaking the sample in the developer solution. Once the pattern was ready, 200 nm thick aluminum metal was deposited using thermal evaporation method and desired metal patterns were achieved after the lift-off process in acetone solution.

To characterize the optical response of the epitaxial grown silicon, we performed the optical-pump-terahertz probe (OPTP) measurements using ZnTe nonlinear crystal based terahertz time-domain spectroscopy (THz-TDS). The thin film of silicon on sapphire (SoS) was independently characterized using OPTP to extract the photoconductivity values of silicon for varying pump fluences. Later the resonant modulation through the device consisting of the hole arrays integrated with the silicon islands is measured using OPTP measurements for the pump beam of wavelengths 400 and 800 nm and the modulation is probed using the THz pulse. The input THz pulse polarized along the *x*-axis (along the shorter length of hole) is used to excite the hole

array sample at its normal incidence. Time dependent electric fields of the THz wave with and without the sample were recorded, which were later converted into frequency domain by Fourier transformation. The normalized THz transmission spectra shown in Figure 2(a) were calculated by normalizing the sample signal ($E_{sample}(\omega)$) with the reference signal ($E_{ref}(\omega)$) as $T(\omega) = \frac{E_{sample}(\omega)}{E_{ref}(\omega)}$. The optical photoexcitation of silicon was achieved using an amplified Ti:sapphire laser which produces optical pulses with 4mJ energy per pulse, at a repetition rate of 1 kHz and a pulse width of ~ 120 *fs* centered at 800 nm. In OPTP measurement the diameter of THz beam was 3 mm and optical pump beam were 10 mm for 800 nm and 5 mm for 400 nm, which ensures homogeneous excitation of the hole array over the area probed by the THz beam. The entire experiment was carried out in the dry nitrogen environment.

Results and Discussion

The experimentally measured transmission spectra from the square hole array are shown in Fig 2(a). Under the normal incidence of the THz wave, the wavelength of SP (Surface-plasmon) resonance through subwavelength metallic square array is given by[11]:

$$\lambda = \frac{p}{\sqrt{m^2 + n^2}} \sqrt{\frac{\varepsilon_{sub}\varepsilon_m}{\varepsilon_{sub} + \varepsilon_m}} \quad (1)$$

where ε_{sub} and $\varepsilon_m = (\varepsilon_{real} + i\varepsilon_{imag})$ are the permittivity of substrate and metal respectively, *p* is the square lattice constant and *m, n* are integers that correspond to specific order of SP mode. As in the THz region, metals satisfy $\varepsilon_{sub} << \varepsilon_{real} << \varepsilon_{imag}$, using this approximation Eq.1 becomes

$$\lambda = \frac{p}{\sqrt{m^2 + n^2}} \sqrt{\varepsilon_{sub}} \quad (2)$$

Eq. 2 is similar to the Wood's anomaly (WA) condition for transmission minima[34]. The detailed derivation from Eq. 1 to Eq. 2 is given in supplementary material.

For our case, [1,0] WA valley occur at 0.8 THz that can be seen in Fig 2(b). However, the experimental spectra (Fig 2(a)) are slightly shifted due to inhomogeneity in the fabricated device. The enhanced transmission through metallic holes is the signature of the existence of surface waves (s*poof plasmon polariton*) as well as localized field across the holes. Photoexciting the silicon by increasing the pump fluence introduces a thin conducting layer, which in turn reduces the scattering efficiency as well as coupling of surface waves to the hole and acts as a subwavelength bridge to tunnel through the hole without scattering[35]. Here, the active tuning of THz transmission was achieved by photoexciting the silicon present in the gap of the hole array. The silicon was photoexcited above the band gap [indirect gap of Si ~ 1.1 eV][33] by 800 nm [E =1.55 eV] femtosecond pulse laser. Figure 2(a) illustrates the experimentally recorded transmission from the sample at various optical pump fluences. As the pump fluences increases from 190 μJ/cm^2 to 1300 μJ/cm^2 the magnitude of terahertz (THz) transmission reduces, which occurs due to the reduced scattering efficiency of surface waves via the holes. Figure 2(b) shows the simulated transmission spectra at different photoconductivity values of silicon. Increasing the photoconductivity in simulation is equivalent to increasing the pump fluence in the experiment. We carried out the simulation by using finite differential time domain (FDTD) method using CST Microwave studio software. In simulation, the unit cell is defined of the same dimension as shown in inset of Figure 1(a), and aluminum metal with reduced conductivity $\sigma = 2.2 \times 10^7$ S/m[36], sapphire ($\varepsilon_r = 11.7$) as transparent substrate and silicon ($\varepsilon_r = 11.9$) as an active material were used. Later the transmission spectra were calculated by applying the unit-cell boundary condition. The photoconductivity values of silicon used in simulation were extracted from THz photoconductivity transmission measurement. In addition to this, the bandwidth of the terahertz transmission can be optimized by changing the dimension or periodicity of the hole arrays.[37]

In supplementary Figure S2 depicts different bandwidth range of terahertz transmission through hole arrays of different dimension.

Color sensitive modulation

Upon illuminating the sample with different wavelengths (in our case 400 nm and 800 nm) but identical fluence exhibits different level of modulation depths. This wavelength dependent modulation provides more controlled and active tuning of THz waves. Figure 3(a) and 3(b) show the experimentally measured transmission spectra, where the hole arrays are optically pumped by 800 and 400 nm light with identical fluences. At each pump fluence, the difference in modulation depths can be seen clearly through Figure 3(a) and 3(b). The contrast is even clearer in the contour plot of transmission (Figure 3(c) and 3(d)). The X and Y axes of contour plot (Figure 3(c) and 3(d)) are frequency and fluence respectively, and the color bar represents the strength of the THz transmission through hole array. Figure 3(c) and 3(d) depict the transmission plot at different pump fluences for 800 nm and 400 nm pump beam. From the plot, we clearly observe that 400 nm pump beam strongly modulates the THz wave compared to 800 nm.

To further illustrate the color dependent modulation, we calculated the magnitude of confined terahertz electric field at resonant frequency across the gap of hole array using CST Microwave studio. Since resonant excitation of surface plasmons creates confined electric fields at the surface which allows light to tunnel through the hole and give rise to resonant transmission, hence the strength of confined terahertz electric field across the hole is directly proportional to the dielectric constant of the medium in the hole. Hence, photoexcitation of epitaxial silicon layer which resides in the hole leads to gradual switch off the resonant transmission through the plasmonic hole array. Figure 4 depicts the magnitude of confined THz electric field across the hole for different photoconductivity values of silicon (Si). Figure 4(a) represents the case where the sample does not undergo any photoexcitation, while Figure 4(b) and (c) depict the THz confined electric field for 800 and 400 nm optical excitation at pump fluence of 265 $\mu J/cm^2$. To

simulate this, we assigned the experimentally extracted photoconductivity (Figure 5(a)) values to silicon, where σ = 0 S/m represents the no pumping case, while σ = 3500 S/m and 14000 S/m correspond to the photoconductivity of silicon for the 800 nm and 400 nm pump beam excitation respectively with pump fluence of 265 μJ/cm^2.

The difference in modulation arises because different wavelength pump beams with identical fluences generate different number density of photocarriers. To validate this, we measured the photoconductivity of unpatterned silicon epitaxial layer at frequency f =0.71 THz at identical fluences using 800 nm and 400 nm pump beams, as photoconductivity is directly proportional to the free carrier number density. Figure 5(a) represents the experimentally extracted photoconductivity value for silicon by using 400 nm and 800 nm pump beam at identical fluences. The detailed explanation of the extraction of photoconductivity is given in the supporting information. The higher photoconductive values for 400 nm clearly supports the fact that charge carrier generation is higher compare to 800 nm pump beam. The modulation depth of the hole array resonance in the presence of the pump beam of different is calculated as, $\text{Modulation} = \frac{|T_{No\ pump} - T_{pump}|}{T_{No\ pump}} \times 100\ \%$. Figure 5(b) depicts the modulation of terahertz transmission at resonant frequency (f = 0.71 THz) with various pump fluences. The spectral modulation depths at other frequencies are shown in supporting information (Figure S1). At each fluence, 400 nm optical pump beam largely modulates the THz transmission compared to 800 nm, which arises due to large photocarrier generation by 400 nm beam. In addition to this, Figure 5(b) illustrates the comparison of modulation achieved using 400 and 800 nm pump beams. From the figure it is clear that, the identical modulation depth can be achieved by 400 nm pump beam at lower pump fluence. For example, almost 60 % modulation can be achieved by 400 nm pump beam at 200 μJ/cm^2 pump fluence compare to 800 nm pump beam with 500 μJ/cm^2 pump fluence. This comparative study allows us to selectively choose the pump

wavelength to achieve a specific modulation depth, particularly in such applications that require extremely low fluence operation.

Conclusion

In summary, we have demonstrated the color dependent active modulation of terahertz transmission via subwavelength metal hole arrays fabricated on epitaxial silicon film. Photoexciting the silicon with different wavelength modulates the terahertz wave with contrasting modulation depths and different ultrafast switching time. Photoexcitation with different colored femtosecond pulse exhibits different carrier relaxation time which could be easily exploited for ultrafast switching applications. Thus, controlling the terahertz wave (THz) waves by using different wavelength pump beam provides an extra degree of freedom which would pave new path in controlling and guiding the terahertz waves for various applications like terahertz imaging, sensing, and high-speed communication. Such a color dependent investigation would have tremendous significance in novel quantum semiconducting material systems where slight change in color of the photoexcitation could lead to super high speed devices that could be switched with extremely low power of incident light.

Acknowledgment

The authors acknowledge the Singapore Ministry of Education Grant No. MOE2015-T2-2-103 for funding of this research.

References

[1] M. Tonouchi, Nat Photon 2007, 1, 97.
[2] N. K. Grady, J. E. Heyes, D. R. Chowdhury, Y. Zeng, M. T. Reiten, A. K. Azad, A. J. Taylor, D. A. R. Dalvit, H.-T. Chen, Science 2013, 340, 1304.
[3] N. I. Landy, C. M. Bingham, T. Tyler, N. Jokerst, D. R. Smith, W. J. Padilla, Physical Review B 2009, 79, 125104.
[4] A. Degiron, H. J. Lezec, W. L. Barnes, T. W. Ebbesen, Applied Physics Letters 2002, 81, 4327.
[5] J. Bravo-Abad, A. Degiron, F. Przybilla, C. Genet, F. J. Garcia-Vidal, L. Martin-Moreno, T. W. Ebbesen, Nat Phys 2006, 2, 120.
[6] L. Martín-Moreno, F. J. García-Vidal, H. J. Lezec, K. M. Pellerin, T. Thio, J. B. Pendry, T. W. Ebbesen, Physical Review Letters 2001, 86, 1114.
[7] A. Mary, S. G. Rodrigo, L. Martín-Moreno, F. J. García-Vidal, Physical Review B 2007, 76, 195414.
[8] A. K. Sarychev, V. A. Podolskiy, A. M. Dykhne, V. M. Shalaev, IEEE Journal of Quantum Electronics 2002, 38, 956.
[9] A. V. Zayats, L. Salomon, F. De Fornel, Journal of Microscopy 2003, 210, 344.
[10] A. K. Azad, W. Zhang, Opt. Lett. 2005, 30, 2945.
[11] Y. Yang, D. R. Grischkowsky, IEEE Transactions on Terahertz Science and Technology 2013, 3, 151.
[12] S.-H. Chang, S. K. Gray, G. C. Schatz, Opt. Express 2005, 13, 3150.
[13] W. L. Barnes, W. A. Murray, J. Dintinger, E. Devaux, T. W. Ebbesen, Physical Review Letters 2004, 92, 107401.
[14] K. J. K. Koerkamp, S. Enoch, F. B. Segerink, N. F. van Hulst, L. Kuipers, Physical Review Letters 2004, 92, 183901.
[15] A. Degiron, T. W. Ebbesen, Journal of Optics A: Pure and Applied Optics 2005, 7, S90.
[16] Y.-H. Ye, J.-Y. Zhang, Opt. Lett. 2005, 30, 1521.
[17] D. Qu, D. Grischkowsky, W. Zhang, Opt. Lett. 2004, 29, 896.
[18] C. Genet, T. W. Ebbesen, Nature 2007, 445, 39.
[19] J. B. Pendry, L. Martín-Moreno, F. J. Garcia-Vidal, Science 2004, 305, 847.
[20] F. J. García de Abajo, J. J. Sáenz, Physical Review Letters 2005, 95, 233901.
[21] L. Shen, X. Chen, T.-J. Yang, Opt. Express 2008, 16, 3326.
[22] A. P. Hibbins, B. R. Evans, J. R. Sambles, Science 2005, 308, 670.
[23] F. J. Garcia-Vidal, L. Martín-Moreno, J. B. Pendry, Journal of Optics A: Pure and Applied Optics 2005, 7, S97.
[24] S. A. Maier, S. R. Andrews, L. Martín-Moreno, F. J. García-Vidal, Physical Review Letters 2006, 97, 176805.
[25] W. L. Barnes, A. Dereux, T. W. Ebbesen, Nature 2003, 424, 824.
[26] J. A. H. van Nieuwstadt, M. Sandtke, R. H. Harmsen, F. B. Segerink, J. C. Prangsma, S. Enoch, L. Kuipers, Physical Review Letters 2006, 97, 146102.
[27] H.-T. Chen, W. J. Padilla, J. M. O. Zide, A. C. Gossard, A. J. Taylor, R. D. Averitt, Nature 2006, 444, 597.
[28] A. K. Azad, H.-T. Chen, S. R. Kasarla, A. J. Taylor, Z. Tian, X. Lu, W. Zhang, H. Lu, A. C. Gossard, J. F. O'Hara, Applied Physics Letters 2009, 95, 011105.
[29] H. Tao, A. C. Strikwerda, K. Fan, W. J. Padilla, X. Zhang, R. D. Averitt, Physical Review Letters 2009, 103, 147401.
[30] H.-T. Chen, J. F. O'Hara, A. K. Azad, A. J. Taylor, R. D. Averitt, D. B. Shrekenhamer, W. J. Padilla, Nat Photon 2008, 2, 295.
[31] T. Driscoll, H.-T. Kim, B.-G. Chae, B.-J. Kim, Y.-W. Lee, N. M. Jokerst, S. Palit, D. R. Smith, M. Di Ventra, D. N. Basov, Science 2009, 325, 1518.
[32] H.-T. Chen, W. J. Padilla, M. J. Cich, A. K. Azad, R. D. Averitt, A. J. Taylor, Nat Photon 2009, 3, 148.
[33] G. E. J. Jr., F. A. Modine, Applied Physics Letters 1982, 41, 180.
[34] Proceedings of the Royal Society of London. Series A 1907, 79, 399.
[35] E. Hendry, M. J. Lockyear, J. Gómez Rivas, L. Kuipers, M. Bonn, Physical Review B 2007, 75, 235305.

[36] N. Laman, D. Grischkowsky, Applied Physics Letters 2007, 90, 122115.
[37] F. J. García-Vidal, E. Moreno, J. A. Porto, L. Martín-Moreno, Physical Review Letters 2005, 95, 103901.

Figures

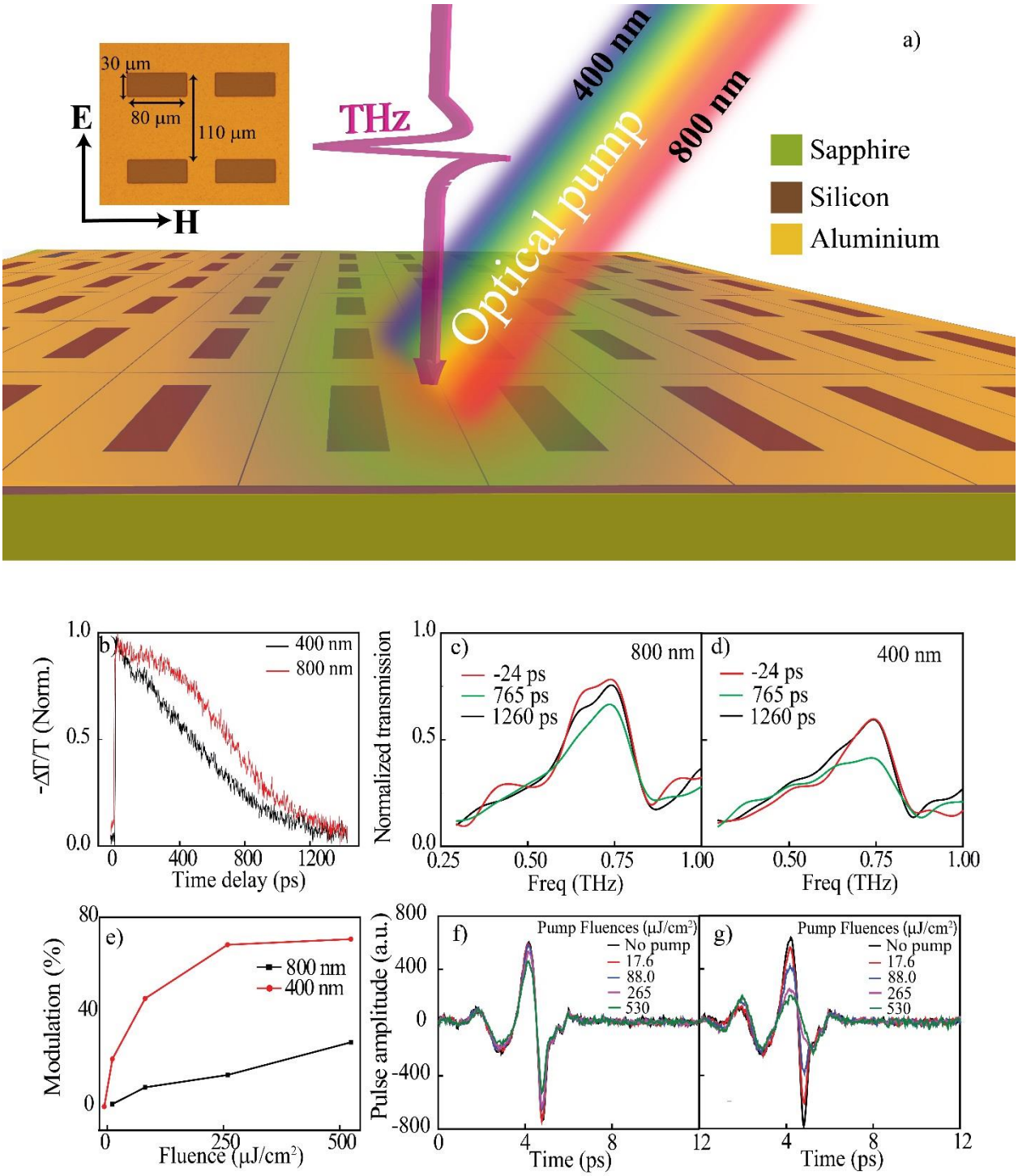

Figure 1. a) Graphical representation of the hole arrays sample excited by optical pump beam and probed by THz. The different color of optical pump beam represents the color sensitive nature of the hole arrays. Inset shows optical microscope image of sample with dimensions (a_x = 30 μm, a_y = 80 μm and periodicity $p_x = p_y$ = 110 μm) **b)** Charge carrier relaxation dynamics in silicon thin film. **c) and d)** Terahertz transmission through hole array at different pump and probe delay time (τ_p), where figure (c) and (d) represent 800 nm and 400 nm optical excitation respectively. **e)** Experimentally measured modulation of transmitted THz time signal at different pump fluence for

400 nm (blue-solid-circles) and 800 nm (red-solid-squares) optical excitation. **f) and g)** Transmitted terahertz time signal through hole array at various pump fluences for λ = 800 nm (Figure 1(f)) and λ = 400 nm (Figure 1(g)) optical excitation.

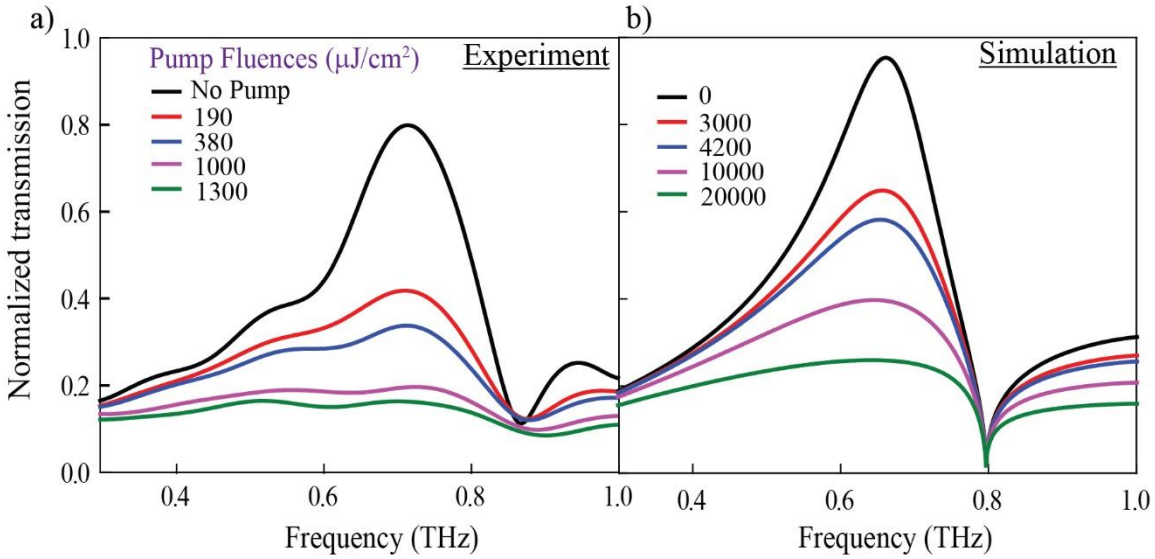

Figure 2. **a)** Experimentally measured transmission spectra through hole array at various pump fluences of 800 nm light. **b)** Simulated transmission spectra of the hole array at different photoconductivity values of silicon (Si)

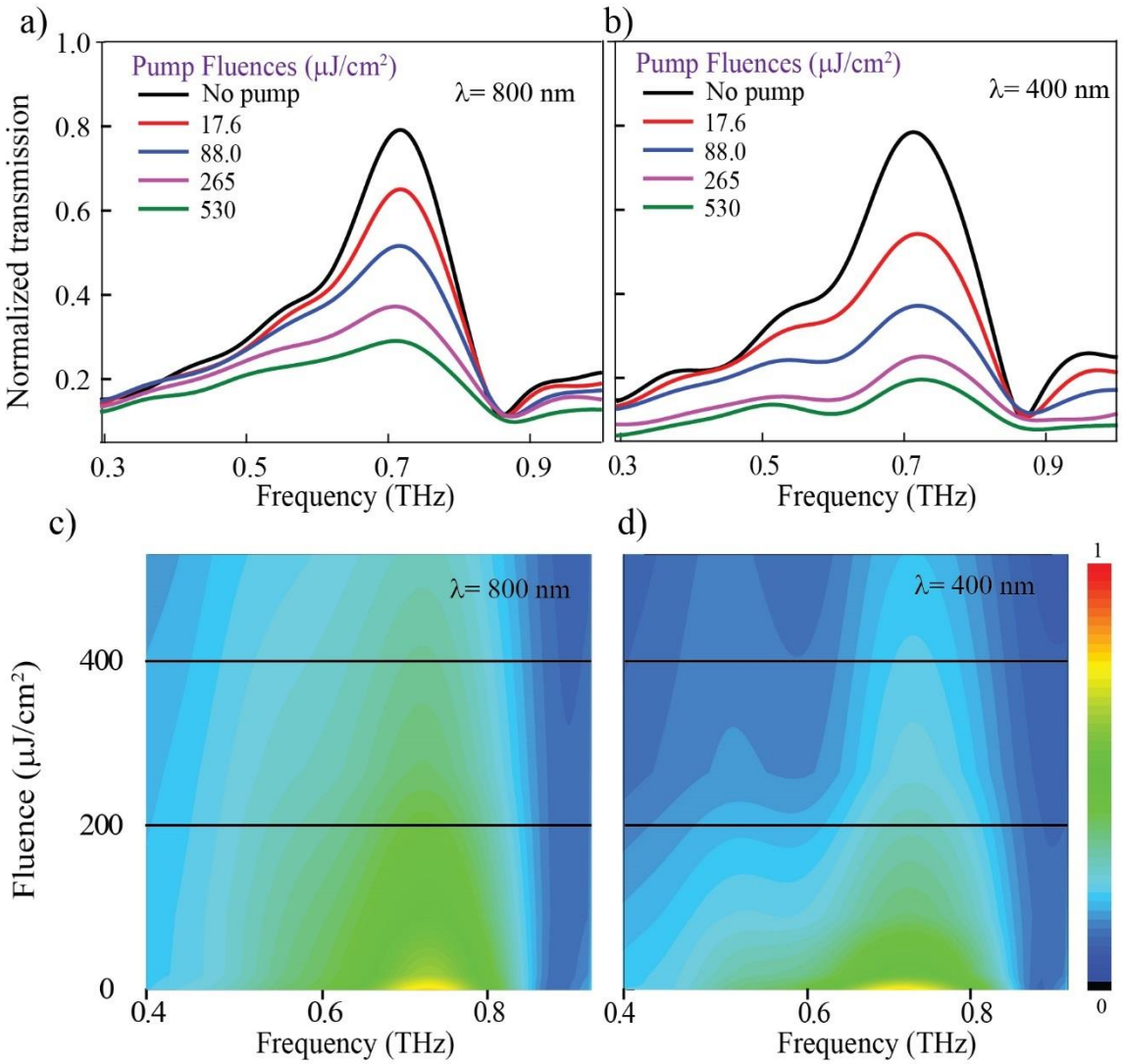

Figure 3 a,b) Experimentally measured THz transmission from hole arrays at various optical pump fluences. In case a) and b) optical pump with wavelength 800 nm and 400 nm were used respectively. **c,d)** Contour plot of THz transmission at various optical pump fluences as a function of frequency. In case c) and d) optical pump with wavelength 800 nm and 400 nm were used respectively. The horizontal solid black lines are drawn at pump fluences 400 and 200 (μJ/cm²) to compare the THz transmission.

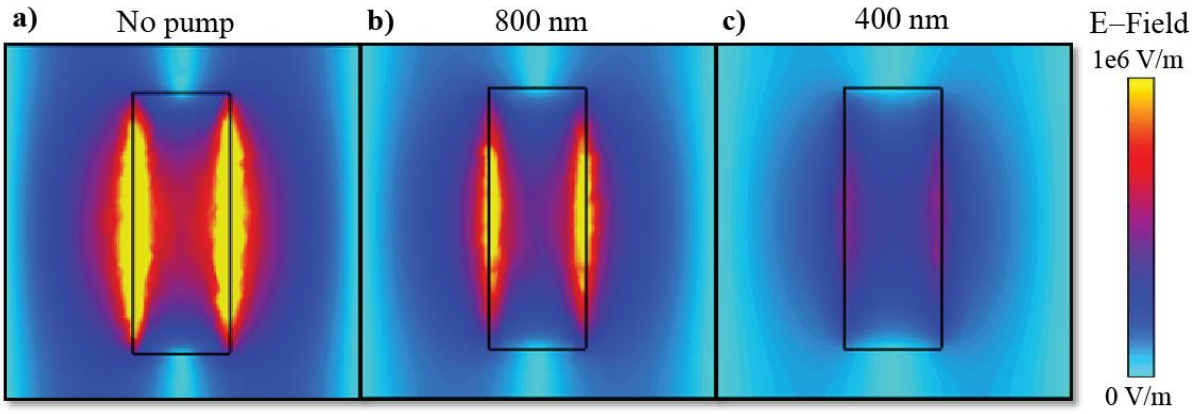

Figure 4 Terahertz electric field confinement across the hole at resonant frequency (f = 0.71 THz) for different wavelength optical excitation **a)** E-field confinement for no pump i.e. σ = 0 S/m **b)** E-field confinement for 800 nm optical pump excitation with pump fluence of 265 μJ/cm^2. In this case the photoconductivity of Si is σ = 0 S/m (Figure 5(a)) **c)** E-field confinement for 400 nm optical pump excitation with pump fluence of 265 μJ/cm^2. In this case the photoconductivity of Si is σ = 14000 S/m (Figure 5(a))

Figure 5. a) Photoconductive values of 600 nm thick silicon epilayer at various pump fluences by 400 nm (blue

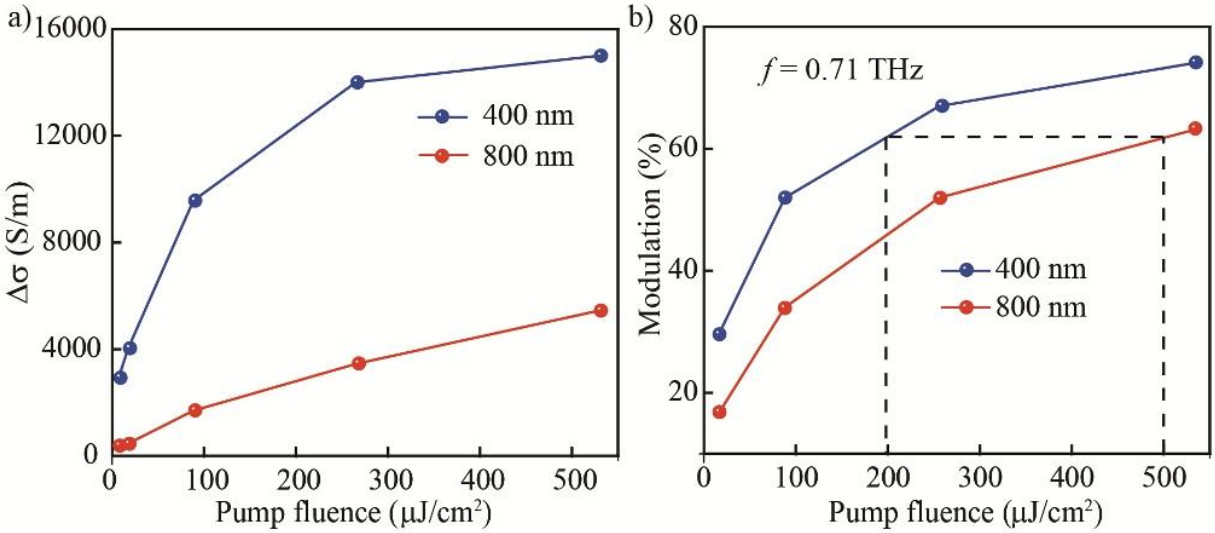

line) and 800 nm (red line) optical pump beam. The photoconductivity is calculated using OPTP measurements (details are given in Supplementary information). **b)** Comparison of modulation by 400 nm (blue curve) and 800 nm (red curve) pump beam at peak transmission value (f = 0.71 THz) of the plasmonic hole array.